

Predicting the Pressure Drop of Corrugated Sheet Structured Packings in Deep Vacuum Applications



This work is licensed under a Creative Commons Attribution 4.0 International License

<https://doi.org/10.15255/CABEQ.2018.1574>

Original scientific paper

Received: December 31, 2018

Accepted: September 24, 2019

Ž. Olujic*

Retired, the Netherlands

Advanced corrugated sheet structured packings are considered a natural choice for deep vacuum distillation. In many of these applications that occur at absolute pressures below 0.01 bar at the top of the column, the low density gas/vapor driven by pressure ascends through an irrigated packed bed under laminar flow conditions. This implies that the packing geometry features aiming to reduce the form drag of advanced packing may not be as effective, if at all, as experienced in common applications where turbulent flow prevails. To consider this appropriately, a theoretically founded expression for laminar flow friction factor has been incorporated into Delft model (DM). With this extension, the predicted pressure drop within laminar flow region approaches closely that estimated using well-established empirical model available in software package SULCOL. In absence of adequate experimental evidence, extended DM was validated using newest data obtained at FRI with an advanced wire gauze structured packing in total reflux experiments carried out with paraxylene/orthoxylyene system at 0.02 and 0.1 bar top pressure in a column with internal diameter of 1.22 m.

Keywords:

distillation, packed columns, structured packings, pressure drop

Introduction

In a paper presented at AIChE Spring Meeting held in 2013 in San Antonio, TX, USA, Duss¹ has indicated a number of industrially important deep vacuum applications of structured packing with gas or vapor phase ascending under laminar flow conditions. To the most extreme operation in this respect belongs superheated steam stripping of free fatty acids (FFA) and other valuable impurities as well as some contaminants from raw edible oils (operating pressure: 0.001 – 0.003 bar at the top), and subsequent separations of various fatty acids and other valuable high-boiling chemicals by multistage fractionation at top absolute pressures well below 0.01 bar². Although these pressures are considered rather high in terms of vacuum technology nomenclature, in technical literature these stripping and distillation operations are generally referred to as deep vacuum applications.

Indeed, performance of corrugated sheet structured packings in conventional absorption, distillation, and stripping applications is well understood and reliable methods exists to predict their performance. However, nothing of existing knowledge is of direct use when a structured packing is considered for deep vacuum applications. An evaluation

of predictive methods for pressure drop of structured packings, available in software packages of a number of packing manufacturers, reported recently by Duss¹, has indicated that most of these purely empirical methods rely on constant values of an overall drag coefficient, usually determined from measurements conducted under turbulent gas flow conditions. As such, these tend to underpredict strongly the pressure drop when applied to laminar flow range.

An exception in this respect is the pressure drop estimation method available in Sulzer package SULPAK^{1,3}. It makes a distinction between laminar and turbulent flow regions, and accounts for observed packing-type- and size-related effects by using adequate, experimentally validated values of the characteristic drag coefficient. This is of crucial importance, because under laminar flow conditions, the internal fluid friction is the governing factor, while a gas or vapor ascending through an irrigated packed bed under turbulent flow conditions experiences a considerable amount of additional pressure loss due to various manifestations of form drag.

A more generic, insight-providing approach, is that based on Delft Model (DM)^{4,5}, which requires no packing-specific parameter to predict pressure drop of a corrugated sheet structured packing in common applications. To improve model reliability and cover appropriately the process conditions as

*Corresponding author: E-mail: zarko.olujic@hotmail.com

encountered in deep vacuum, low gas or vapor density applications, a theoretically founded expression for laminar flow friction has been incorporated into DM. As shown in this study, with this extension, predictions of DM closely approach those of SULCOL within laminar and transition flow range, indicating that pressure drop of corrugated sheet structured packings can be modelled with confidence and sufficient accuracy in a theoretically founded way.

Previous work

On predictive models side, pure empirics prevail, in spite of the fact that firm theoretical foundations for a physically sound approach to modelling the fluid dynamics and mass transfer in an irrigated packed bed had been laid shortly after industrial introduction of corrugated sheet structured packing made of wire gauze by SULZER in mid 1960s⁶. In early 1970s, Zogg^{7,8} published the results of his fluid-dynamics studies carried out with Sulzer BX wire gauze packing with different corrugation inclination angles, indicating that transition from laminar to turbulent flow regime occurs at much lower gas Reynolds numbers than is the case with fluid flow through straight tubes ($Re_G \cong 2300$). According to Zogg^{7,8}, the critical Reynolds number for packing with corrugation inclination angle of 60° with respect to horizontal axis (30° or X packing according to Sulzer nomenclature) is around 300, while that of BX packing with common 45° is around 200. Outgoing from interpretation of experiments that have generated these numbers, Duss¹ arrives at 250 as critical Reynolds number for all 45° packings, and 450 for all 60° packings. Note that, in the case of a 45° packing, the change in flow direction at transitions between subsequent packing layers is much sharper (90° vs 120°), and this induces occurrence of turbulence at a lower vapor velocity than is the case with a smoother transition, like in the case of X packings and advanced packing forms (MellapakPlus and BXPlus) with smooth bends at both ends of corrugations. The aforementioned critical Reynolds numbers are generally valid for industrial scale column diameters, i.e., those where the ratio of column diameter and the hydraulic diameter of the packing considered is larger than 100¹⁰.

SULCOL pressure drop model

All macro geometry related effects are accounted for accordingly in pressure drop model available in Sulzer's software package SULCOL⁹ by using adequate, experimentally validated values of the characteristic drag coefficient, in conjunction with a simple general equation describing the pressure drop per unit bed height^{1,3}:

$$\frac{\Delta p}{\Delta z} = \frac{c_f}{d_{hG,V}} \frac{\rho_G u_{Gs}^2}{2} = \frac{c_f}{d_{hG,V}} \frac{F_{Gs}^2}{2} \quad (1)$$

where Δp (mbar) is pressure drop or loss, Δz (m) represents the packed bed height or depth, c_f (–) is the characteristic drag coefficient, ρ_G (kg m^{-3}) is gas or vapor density, u_{Gs} (m s^{-1}) is superficial gas velocity, and F_{Gs} ($\text{Pa}^{0.5}$) is gas or vapor load, often called the F-factor, based on superficial gas velocity: $F_{Gs} = u_{Gs} \rho_G^{0.5}$.

The hydraulic diameter of the V-shaped gas flow channel, $d_{hG,V}$ (m), corresponds with the length of the corrugation side, s (m):

$$d_{hG,V} = \frac{4}{a_p} = s \quad (2)$$

where a_p ($\text{m}^2 \text{m}^{-3}$) is the specific geometric area of the packing.

Eq. (1) relates pressure drop to superficial gas velocity and the packed bed height, and the hydraulic diameter is that of dry packing. Under common operating conditions, the gas ascends through an irrigated packed bed along a flow path that is substantially longer than the bed height, and at an effective velocity that is significantly higher than the superficial gas velocity, in both cases to the extent depending on corrugation inclination angle. In other words, the pressure drop causing effects related to the effective gas velocity, actual gas flow path length and effective porosity, as well as all other form drag related losses are lumped together in the characteristic value of the packing type and size-dependent specific drag coefficient. The latter is available for each type and size of Sulzer structured packings in SULCOL data bank as a function of gas or vapor Reynolds number, Re_{Gs} (–), based on superficial gas or vapor velocity, defined as

$$Re_{Gs} = \frac{u_{Gs} \rho_G d_{hG,V}}{\mu_G} \quad (3)$$

In general, Eq. (1) with adequate drag-coefficient values captures correctly pressure drop trends and generates reasonable pressure drop values, and holds generally for column diameters above 1 m. Useful information and hints how to evaluate and ascertain that SULCOL will be used appropriately in cases where gas densities are below 0.1 kg m^{-3} can be found in closing remarks of Duss paper¹. A concise and consistent view on performance characteristics of structured packings and auxiliary equipment in general, including hydraulics, can be found in a book chapter written by Spiegel and Duss¹⁰.

Table 1 – Fixed and variable parameters of the hypothetical operating conditions base case¹ considered in this study

Fixed	ρ_G (kg m ⁻³)	u_{Gs} (m s ⁻¹)	ρ_G (kg m ⁻³)	u_{Gs} (m s ⁻¹)
ρ_L (kg m ⁻³)	800	0.002	44.7	0.2
μ_L (Pa s)	0.0002	0.005	28.3	0.5
μ_G (Pa s)	0.00001	0.01	20.0	1
σ (N m ⁻¹)	0.02	0.02	14.1	2
u_L (m ³ m ⁻² h ⁻¹)	2	0.05	8.9	5
F_G (Pa ^{0.5})	2	0.1	6.3	

Base case and packings considered

Table 1 shows relevant information concerning the hypothetical operating conditions base case used by Duss¹ to demonstrate usability of SULCOL pressure drop method in deep vacuum applications covering laminar, transient, and turbulent regions of gas or vapor flow. A typical fixed specific liquid load was chosen, as well as vapor and liquid viscosities. The chosen value of the vapor load or F-factor was constant, while densities and velocities of gas or vapor have been arranged accordingly to cover the whole range of operation, including deep vacuum distillation conditions.

This was done in conjunction with two Sulzer high performance structured packings, well established in deep vacuum applications, i.e. BXPlus and MellapakPlus 252.Y¹. To get a complete picture, the present study includes also two conventional counterparts of the latter, Mellapak 250.Y (45°) and Mellapak 250.X (60°, with respect to horizontal)¹¹.

Nominal specific geometric area of MellapakPlus 252.Y is ~ 250 m² m⁻³, and the hydraulic diameter is 0.016 m, while the hydraulic diameter of the BXPlus packing with factor two larger specific geometric area is a half of that of MellapakPlus 252.Y ($a_p \sim 500$ m² m⁻³, $d_{hG} = 0.008$ m). MellapakPlus 252.Y is the advanced version of conventional Mellapak 250.Y, with corrugations inclined by 45° and both ends of corrugations smoothly bent to the vertical. In addition, both ends of corrugations of the wire gauze BXPlus packing are bent to vertical, and the corrugation inclination angle of this packing as well as of its conventional counterpart BX is 60°.

SULCOL pressure drop estimates for the base case

The drag coefficients for Mellapak 250.Y, Mellapak 250.X, MellapakPlus 252.Y, and BXPlus for the conditions indicated in Table 1 are shown in Fig. 1 as a function of Reynolds number. All four

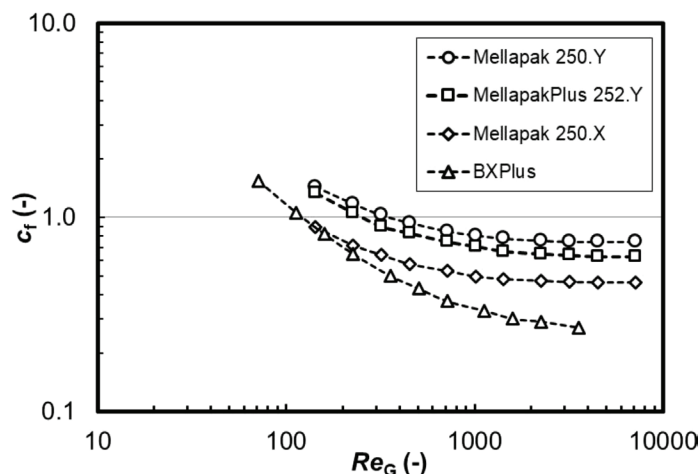


Fig. 1 – Drag coefficient as a function of gas or vapor Reynolds number for four representative different types and sizes of Sulzer corrugated sheet structured packings in conjunction with hypothetical operating conditions base case, with fixed values of vapor load, liquid load, vapor viscosity, and liquid properties (see Table 1), considered in this study^{1,11}

curves exhibit similar trend, and tend to flatten with increasing Reynolds number, indicating a gradual transition from laminar to turbulent flow, but differ in absolute values to the extent depending on distinctive macro geometric features, i.e., corrugation inclination angle and hydraulic diameter. Since the Reynolds number depends on the hydraulic diameter of the packing, the drag coefficient curve of BXPlus at the same operating conditions lies below that of the three Mellapak types with a specific geometric area of 250 m² m⁻³. Therefore, it is shifted to the left accordingly, indicating a pronouncedly steeper increase with decreasing Re-number within laminar flow region.

Corresponding pressure drop curves are shown in Fig. 2, indicating the same trend. Since the product of density and the square of the superficial gas velocity in Eq. (1) is constant, the pressure drop curve reflects that of the characteristic drag coefficient, exhibiting a decreasing pressure drop with increasing Reynolds number. Due to a factor 2 smaller hydraulic diameter, the position of BXPlus curve has changed with respect to that of the corresponding drag coefficient (Fig. 1).

One should note here that the trend of the pressure drop curves shown in Fig. 2 deviates from common pressure drop behavior, because the operating conditions used to create Fig. 2 were specifically adapted to keep the F-factor constant for all indicated points. Namely, in industrial applications, pressure drop is estimated for a number of relevant points along the column, most typically for top and bottom of the rectification and stripping sections. The operating conditions, including vapor and liquid throughputs, are fixed at these positions and a change in diameter (during design phase) will result

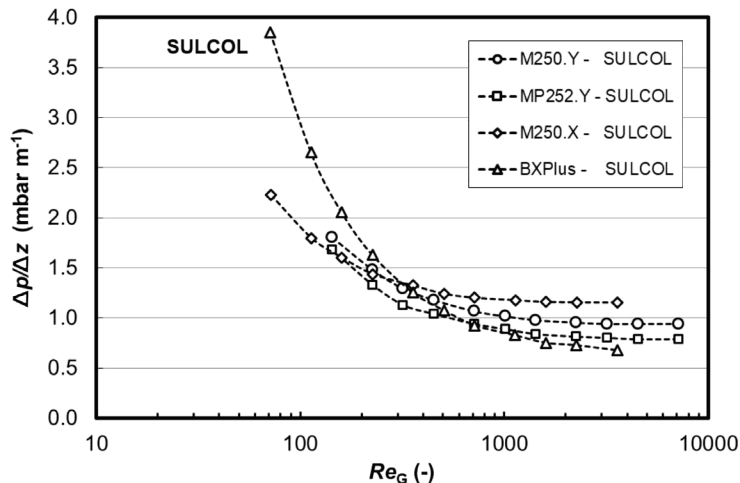


Fig. 2 – Specific pressure drop curves as estimated by SULCOL using drag coefficient values shown in Fig. 1

in a change in pressure drop, because gas or vapor velocity will change accordingly. Experimental evaluation of the hydraulic performance of structured or random packings and trays for distillation purposes is usually carried out in columns with given diameter using air-water system at ambient conditions or established binary organic mixtures in conjunction with total reflux distillation tests. In the former case, experiments are usually carried out for a fixed liquid load, starting from lowest reasonable gas load to that causing hydraulic flood of the test column. In these tests, increasing gas throughput results in correspondingly increasing gas velocity and, consequently, increasing Reynolds number. A similar situation is with total reflux distillation tests, where with increasing vapor and liquid throughput, corresponding superficial gas and liquid velocities as well as gas or vapor phase Reynolds number increase accordingly. In other words, under common processing and equipment testing conditions, the pressure drop of structured packings tends to increase with increasing gas or vapor phase Reynolds number.

However, the present case, using hypothetical operating conditions, where the vapor load (F-factor) is fixed and gas or vapor density and superficial velocity varied accordingly, allows indication of the behavior of pressure drop estimation method over the whole range of operating conditions, including the unexplored field of so-called deep vacuum applications, characterized by very low gas or vapor density, which assumes values well below 0.05 kg m^{-3} . The latter is a good indication of the upper limit for appearance of laminar flow under given processing conditions, while in common vacuum applications, vapor densities are usually above 0.1 kg m^{-3} , and in typical industrial and test situations, often above 1 kg m^{-3} , with Reynolds numbers above 1000, gas or vapor flow is turbulent.

A closer look at the laminar flow region in the graph shown in Fig. 2, demonstrates the essence of the SULCOL empirical pressure drop model, which, for a packing with smaller hydraulic diameter and correspondingly smaller Reynolds number values, indicates a much stronger increase in pressure drop with decreasing Reynolds number compared to coarser packings. This is as expected, because, according to theoretical background, under laminar flow conditions, the pressure drop is proportional to the inverse of the square of the hydraulic diameter of the closed conduit ($\Delta p \approx 1/d_{\text{hG}}^2$), while under turbulent conditions, the hydraulic diameter effect is much less pronounced, i.e., $\Delta p \approx 1/d_{\text{hG}}^{1.25}$. However, one should note that absolute values of the estimated specific pressure drop at Reynolds numbers below 500, going up to 3 mbar m^{-1} , are rather high, i.e., beyond those that could be tolerated in deep vacuum applications. This is a consequence of the choice of given constant value for vapor load, i.e., F-factor ($F_G = 2 \text{ Pa}^{0.5}$), which is approximately by a factor four larger than those encountered, for instance, in edible oil stripping operations. Namely, chosen very low values for gas or vapor densities are realistic, and the wrongdoer in this hypothetical case are too high superficial gas or vapor velocities needed to maintain the value of given F-factor constant.

On the other hand, if we consider the turbulent region, it appears that the pressure drop of BXPlus packing is lower than that of MP252.Y, a packing with factor 2 smaller specific geometric area, i.e., a factor 2 larger hydraulic diameter. This indicates that the pressure-drop reduction effect of corrugation inclination-angle increase from 45 to 60 degrees in the present case outweighs the pressure drop increasing effect of a factor 2 reduction in the hydraulic diameter. As expected, in case of the same corrugation inclination angle (BXPlus vs. M250.X), the pressure drop of packing with larger specific geometric area is higher.

A comparison of M250.Y and M250.X data indicates that the difference in estimated pressure drop is equal for both laminar and turbulent flow conditions, that of 45° packing being factor 1.62 (on average) larger over the whole range of vapor phase Reynolds number than that of 60° packing with the same specific geometric area. This may be considered as anomalous, because under turbulent flow conditions, in addition to the frictional losses, a substantial amount of pressure drop is created by form drag, i.e., flow direction change and related phenomena, which strongly depends on corrugation inclination angle. This means that above number, which reflects a situation under laminar flow conditions should be larger, i.e. factor 2 or more under turbulent flow conditions.

Namely, if we assume that under laminar flow conditions the pressure drop is generated by friction only, then the given factor reflects the difference in the length of flow path and effective vapor velocity as imposed by the difference in corrugation inclination angle for the same bed height and operating conditions. Assuming that ascending vapor flows along V-shaped flow channel, the difference in flow path length corresponds with the ratio of sines of flow direction angles ($\sin 45^\circ / \sin 60^\circ = 1.225$). With both the effective flow path length and effective velocity larger by factor 1.225, the pressure drop in case of Y packing should be within laminar flow region factor 1.5 larger than that of X packing. Given value (1.62) is some 8 % larger, which could be expected due to certain contribution of friction of crossing vapor flows along a flow channel within a packing layer, and entrance effects at transitions between packing layers where flow direction change occurs. Upon entering the turbulent flow region, the ascending vapor, as mentioned previously, experiences direct losses due to flow direction change, which occurs at much sharper angle in case of Y packing (90°) than X packing (120°).

If we consider the relative performance of conventional (Mellapak 250.Y) and advanced (MellapakPlus 252.Y) geometries, then it appears that the same packing with smooth bends on both ends of corrugations reduces the pressure drop from 7 to 10 % within laminar region, and this difference tends to increase with increasing Re number to about 20 % within turbulent flow region. Indeed, an increased reduction in pressure drop may be expected within turbulent flow region, because at transitions between packing layers, a sharp flow direction change is transformed into a smooth one. This also positively affects the transition from layer to layer under laminar flow conditions, but to a lesser extent than under turbulent flow conditions, and this is correctly reflected by SULCOL.

Summarizing, the practical strength of empirical pressure drop model employed within SULCOL lies in its simplicity, and the fact that the key parameter, the drag coefficient c_f (–), can simply be back-calculated from measured pressure drop values using Eq. (1). The characteristic drag coefficient values are available in SULCOL for all types and sizes of Sulzer structured packings, and can only with approximation be applied to similar packings from other vendors.

Delft model extension

A more detailed and insight-providing approach is to make use of a generic type of predictive pressure drop model, i.e., a model that relies on basic

corrugation dimensions of structured packings and is capable of estimating pressure drop without using a packing-specific empirical parameter. This is the main characteristic and added value of the so-called Delft model (DM), which includes a number of fundamentally sound, and, where needed, experimentally substantiated empirical expressions describing all relevant quantities and variables. It was introduced more than 20 years ago, and in the mass transfer part, it includes the laminar flow related correlation, while the corresponding friction factor, at that time considered practically irrelevant, was omitted⁴. However, this was not at the cost of model reliability, because, as shown later, other provisions built in the hydraulic part of the DM account for the steeper increase in pressure drop within laminar flow regime, but as observed during evaluation of a few proprietary experimental deep vacuum data ($Re_G < 100$), this appeared to be insufficient.

The present paper provides an appropriate solution in this respect. By adopting a theoretically founded model for frictional pressure drop of structured packings under laminar gas flow conditions, the validity of DM has been extended to cover fully the range of most extreme operating conditions encountered under deep vacuum conditions in industrial practice. To avoid misunderstandings and erroneous use, the following section provides all relevant expressions, including laminar friction extension, with accompanying background descriptions.

In order to refresh the related basic knowledge, Fig. 3 shows a photograph of a packed bed consisting of five layers of a corrugated sheet structured packing. Each layer is rotated by 90° to the previous one. As illustrated in attached drawing, this arrangement forces pressure difference driven ascending gas or vapor to follow a zig-zag flow path, with a sudden change in flow direction at each transition between packing layers. This causes pressure loss, to the extent depending on flow regime and flow channel inclination angle. Each packing layer or element consists of a multiplicity of short, inclined V-shaped flow channels open on crossings with channels from neighboring corrugated sheet oriented in opposite direction. This basic flow channel structure is shown schematically in Fig. 4, including a drawing of a V-shaped gas or vapor flow channel cross-section with all pertinent flow channel geometry and liquid film specific parameters indicated.

As indicated in the drawing, descending liquid driven by gravity tends to flow under a steeper angle than the corrugation inclination angle, and similar to ascending gas flow, its flow path length tends to decrease with increasing corrugation inclination angle. This means that the extent of gas-liquid interaction, i.e., friction at the interface (surface of the

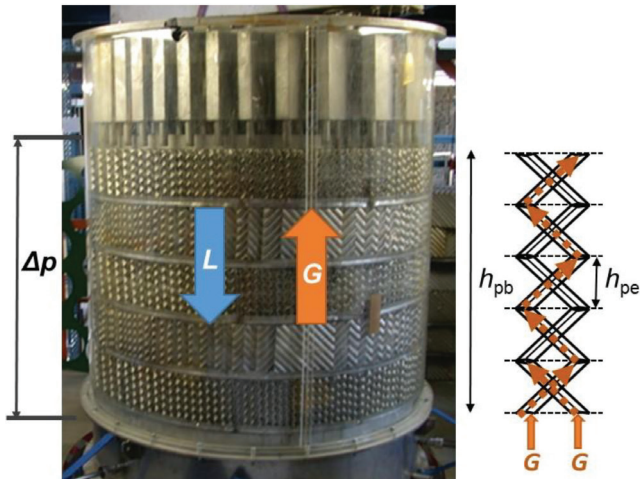


Fig. 3 – Photograph of a packed bed consisting of five layers of corrugated sheet structured packing Montz-pak B1-250, and a sketch illustrating basic flow channel structure forcing the pressure-driven ascending gas or vapor to follow a zigzag flow path

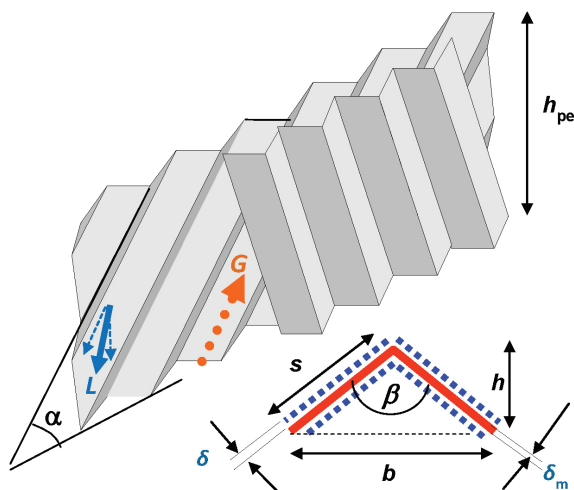


Fig. 4 – Schematic illustration of gas or vapor flow channels formed between neighboring corrugated sheets with oppositely oriented corrugations, with a sketch illustrating basic dimensions of a V-shaped flow channel, where α ($^\circ$) is corrugation inclination angle, β ($^\circ$) is apex or fold angle, b (m) is corrugation base width (perpendicular to gas or vapor flow direction), h (m) corrugation height, s (m) corrugation side length, δ (m) liquid film thickness, δ_m (m) thickness of metal used to make corrugated sheets, and h_{pe} (m) height of a packing element or layer, while G and L indicate direction of pressure-driven ascending gas or vapor flow and gravity-driven descending liquid film flow

liquid film) also depends on the corrugation inclination angle. Furthermore, the packing and liquid holdup occupy a certain amount of packed bed volume, and reduce the cross-sectional area available for gas, forcing it to flow at an effective velocity that is considerably higher than the superficial one, i.e., that based on cross-sectional area of the empty column.

Basic assumptions and working equations of DM

The DM makes a distinction between preloading and loading flow regimes, with loading point as upper limit of preloading region and starting point of the loading region¹². Within preloading region, the specific liquid load is uniformly distributed and complete wetting is assumed, implying a constant film thickness throughout an irrigated packed bed. Upon onset of loading, the liquid starts to build up firstly at transition of packings layers, and at higher gas or vapor loads, parts of descending liquids are blown up through the packing layer, chocking a large number of flow channels, which eventually leads to an inoperable situation, generally known as hydraulic flood.

Regarding the pressure drop behavior, within preloading region with gradually increasing vapor load, the pressure drop tends to increase monotonically, and upon onset of loading, the slope of pressure drop curve becomes much steeper. Therefore, in DM, a distinction is made between preloading and loading regions, and the pressure drop within loading region is expressed by a pressure drop enhancement factor, F_{load} (-), accounting for pressure drop in excess to that corresponding to the preloading region, i.e.:

$$\Delta p = \Delta p_{preload} F_{load} \quad (4)$$

where Δp (Pa or mbar) is overall pressure drop, $\Delta p_{preload}$ (Pa or mbar) is preloading region pressure drop. Pressure drop enhancement factor depends to different extents on gas or vapor load, liquid load, packing porosity, hydraulic diameter of gas flow channel, and corrugation inclination angle, and is estimated using following empirical expression¹²

$$F_{load} = 3.8 \left(\frac{F_G}{F_{G,lp}} \right)^{\frac{2}{\sin \alpha_{DC}}} \left(\frac{u_{Ls}^2}{\varepsilon^2 g d_{hG}} \right)^{0.13} \quad (5)$$

where α_{DC} ($^\circ$) is flow direction change angle, u_{Ls} ($m\ s^{-1}$) is superficial liquid velocity, ε (-) is void fraction or porosity of dry packing, g ($m\ s^{-2}$) is gravity acceleration, d_{hG} (m) is hydraulic diameter of gas or vapor flow channel, and $(F_G/F_{G,lp})$ is the ratio of operating and loading point gas or vapor loads. As long as the value of this ratio is below 1, the liquid holdup is independent of the gas flow rate, and an irrigated packed bed operates under preloading conditions. When the value of this ratio is 1, then the operating gas or vapor load reaches a critical value effecting inception of loading, i.e., initiation of buildup or accumulation of the liquid due to drag exhibited by ascending vapor. Beyond this flow-regime transition point, an irrigated bed operates under fluid-dynamically much more complex

loading conditions, and to estimate related pressure drop, the calculation of pressure-drop enhancement factor in DM is activated. Note that in the case of conventional structured packings, the flow direction change angle is corrugation inclination angle ($\alpha_{DC} = \alpha$).

The characteristic loading point gas or vapor load, $F_{G,lp}$ ($\text{Pa}^{0.5}$), is estimated using a semi-empirical expression that was developed and validated in late 1990s using air/water and total reflux data available at that time in the data bank of Separations Research Program at the University of Texas at Austin^{5,12}. For practical reasons, two slightly different expressions are used, one more suitable for fixed liquid load ($L/G \neq 1$):

$$F_{G,lp} = \left(0.053 \varepsilon^2 g d_{hG} \left(\frac{\rho_L - \rho_G}{\rho_G} \right) \cdot \left(u_{Ls} \sqrt{\frac{\rho_L}{\rho_G}} \right)^{-0.25} \cdot (\sin \alpha_{DC})^{1.24} \right)^{0.57} \cdot \sqrt{\rho_G}$$

(6)

and the other for total reflux ($L/G = 1$) systems:

$$F_{G,lp} = \left(0.053 \varepsilon^2 g d_{hG} (\rho_L - \rho_G) \cdot \left(\frac{u_{Ls}}{u_{Gs}} \sqrt{\frac{\rho_L}{\rho_G}} \right)^{-0.25} \cdot (\sin \alpha_{DC})^{1.15} \right)^{0.5}$$

where ρ_G (kg m^{-3}) and ρ_L (kg m^{-3}) are densities of gas or vapor and the liquid, and α_{DC} ($^\circ$) is angle of gas or vapor flow direction change at the transitions between packing layers. Since in deep vacuum applications very low gas or vapor densities are encountered in conjunction with rather low specific liquid loads, the preloading hydrodynamic conditions prevail. Therefore, the above expressions enabling estimation of loading point and pressure drop enhancement within loading region¹² are of no relevance for considerations related to hypothetical base case mimicking the deep vacuum applications.

Preloading region pressure drop model

As mentioned previously, within preloading region, with the gas or vapor ascending in a zig-zag pattern through an irrigated packed bed consisting of a multiplicity of identical parallel and crossing V-flow channels with the walls covered by a thin liquid film flowing downwardly driven by gravity, there are three dominating sources or components of the total pressure drop, which are accounted for in working expression of Delft Model (DM) for preloading region:

$$\Delta p_{\text{preload}} = (\zeta_{GL} + \zeta_{GG} + \zeta_{DC}) \frac{\rho_G u_{Ge}^2}{2} \quad (8)$$

where u_{Ge} (m s^{-1}) is the effective gas or vapor velocity, and ζ_{GL} ($-$), ζ_{GG} ($-$), ζ_{DC} ($-$) are pressure loss coefficients representing major sources of pressure loss, i.e., those related to gas-liquid friction at the gas-liquid interface (GL), gas-gas interaction (GG), and to the sudden flow direction change (DC) at transitions between packing layers and at the column walls.

One should note, however, that there are also some other, minor sources of pressure loss depending on corrugation inclination angle, which, being relatively small, have not been included explicitly in DM. Namely, due to inclined corrugations, the width of the corrugation base in horizontal plane, i.e., at interface of two packing layers, is larger than the base (perpendicular to axial flow direction) of the triangular or V-shaped flow channel, to the extent depending on corrugation inclination angle ($b' = b/\sin \alpha$). In both cases, gas flow expansion and contraction are gradual and the related loss is relatively small. This occurs at transitions between packing layers and is accompanied by gas flow direction change and related entrance effects. These are reduced significantly in case of advanced versions of corrugated sheet structured packings having both ends, or only lower end of corrugations bent to vertical. Most importantly, the bends also make the transition of descending liquid from one layer to the next layer much smoother, and the vapor load at which loading or liquid build up (accumulation) sets on, is shifted to considerably higher values. In general, the gas flow direction change effect, as a manifestation of form drag, is strong under turbulent flow conditions. Although it can be considered practically negligible under laminar flow conditions, the velocity and axial flow path length variations and velocity profile distortion, as well as more pronounced entrance effects induce certain, relatively small amount of additional pressure loss.

Effective gas or vapor and liquid flow velocities

In an irrigated packed bed with the structure shown in Fig. 3, the gas or vapor phase ascends and the liquid phase descends at a velocity that is significantly higher than the superficial velocity, i.e., that based on the cross-sectional area of an empty column.

Effective gas velocity is defined as

$$u_{Ge} = \frac{u_{Gs}}{(\varepsilon - h_L) \sin \alpha} \quad (9)$$

where u_{Gs} (m s^{-1}) is superficial gas or vapor velocity, ε ($\text{m}^3 \text{m}^{-3}$) is porosity or void fraction of the dry packed bed, h_L ($\text{m}^3 \text{m}^{-3}$) is the liquid holdup, and α ($^\circ$) is corrugation inclination angle with respect to hor-

izontal. While the effective porosity of the irrigated packed bed accounts for the increase in gas velocity due to reduction of cross-sectional area available for gas flow, the gas flow channel inclination angle, α ($^\circ$), dictates the extent of increase in velocity needed to maintain given mean, i.e., superficial gas velocity.

Similarly for the liquid,

$$u_{Le} = \frac{u_{Ls}}{\varepsilon h_L \sin \alpha_L} \quad (10)$$

where u_{Ls} (m s^{-1}) is superficial liquid velocity, and α_L ($^\circ$) is effective liquid flow angle which is always steeper than the corrugation inclination angle.

Assuming that only the gravity and corrugation shape and inclination affect the liquid flow, the effective liquid flow angle, α_L ($^\circ$), can be described by^{4,5,7}:

$$\alpha_L = \arctan \left[\frac{\cos(90^\circ - \alpha)}{\sin(90^\circ - \alpha) \cos \left[\arctan \left(\frac{b}{2h} \right) \right]} \right] \quad (11)$$

where b (m) and h (m) represent corrugation base length and corrugation height, respectively. According to Eq. (11), for corrugated sheet structured packings with corrugation inclination angle of 45° , the liquid driven by gravity will flow under an angle of 54° , while for a 60° packing, the effective liquid flow angle will be 67° .

The ratio $(b/2h)$ indicates the effect of fold or apex angle, which is usually around 90° (e.g.: $b = 2h$). Exception in this respect is corrugated sheet structured packing made of wire gauze, with an apex or fold angle close to 80° . Apex or fold angle (β in Fig. 4) can be determined easily from⁷:

$$\beta = 2 \arctan \left(\frac{b}{2h} \right) \quad (12)$$

The porosity, i.e., void fraction of a dry structured packing bed depends on the thickness of the sheet, δ_m (m), and specific geometric area of the packing a_p , ($\text{m}^2 \text{m}^{-3}$), and can easily be determined from:

$$\varepsilon = 1 - \frac{\delta_m a_p}{2} \quad (13)$$

Nowadays, the common sheet thickness used to manufacture Mellapak and similar packings of other vendors is 0.1 mm, while the average thickness of a corrugated sheet made of wire gauze is around 0.35 mm.

The liquid holdup, h_L ($\text{m}^3 \text{m}^{-3}$), is defined, assuming ideal liquid distribution, i.e., constant liquid film thickness, as a product of the liquid film thickness, δ (m), and the specific geometric area of the packing, a_p ($\text{m}^2 \text{m}^{-3}$)⁴:

$$h_L = \delta a_p \quad (14)$$

This simple basic expression appeared to hold well in practice, in conjunction with well-known Nusselt falling film thickness expression adapted for inclined walls^{4,5}:

$$\delta = \left(\frac{3\mu_L u_{Ls}}{\rho_L g a_p \sin \alpha_L} \right)^{\frac{1}{3}} \quad (15)$$

where g (m s^{-2}) is gravity acceleration, μ_L (Pa s) is the liquid dynamic viscosity, u_{Ls} (m s^{-1}) is superficial liquid velocity, and α_L ($^\circ$) is the effective angle of the liquid film flow.

Gas-liquid and gas-gas friction losses

Basic assumption of Delft Model is that the characteristic gas flow channel has a form of an isosceles triangle with (corrugation) sides covered by flowing thin liquid film, while the open side overlaps with open side of the gas flow channel from neighboring corrugated sheet oriented in opposite direction. The open sides of crossing gas flow channels form a rectangular or a diamond-like plane, where crossing gas streams exhibit shear on each other. Relying on this fact, the necessary condition is fulfilled that allows the “open” side of V-shaped flow channel to be considered as a closed one, which implies that cross-sectional area of the gas or vapor flow channel is that of an isosceles triangle.

The total energy loss due to frictional shear is composed of gas-liquid and gas-gas interaction contributions:

$$\begin{aligned} \zeta_{GL} + \zeta_{GG} &= \left[\varphi \zeta_{GL} + (1 - \varphi) \zeta_{GG} \right] \frac{l_G}{d_{hG,\Delta}} = \\ &= \left[\varphi \zeta_{GL} + (1 - \varphi) \zeta_{GG} \right] \frac{h_{pb}}{d_{hG,\Delta} \sin \alpha} \end{aligned} \quad (16)$$

where φ (–) is the fraction of the perimeter of triangular flow channel covered by liquid film, ζ_{GL} (–) is gas-liquid friction factor, ζ_{GG} (–) is gas-gas friction factor, $d_{hG,\Delta}$ (m) is hydraulic diameter of the triangular gas flow channel, l_G (m) is gas or vapor flow path length. The latter ($l_G = h_{pb}/\sin \alpha$) depends on packed bed height or depth, h_{pb} (m), and corrugation inclination angle, α ($^\circ$). Assuming that gas or vapor flow path will be equal to the total length of inclined flow channels, the latter will be factor 1.225 larger for a conventional packing with corrugation

inclination angle of 45° than that of a packing with corrugation inclination angle of 60° with respect to horizontal.

The fraction of the triangular flow channel perimeter covered by liquid film, φ (–) is:

$$\varphi = \frac{2s}{2s + b} \quad (17)$$

where s (m) is the length of corrugation side, and b (–) is the width of the corrugation base (see Fig. 4).

In the Delft Model, as mentioned previously, the hydraulic diameter is based on a (closed) triangular channel. For a dry triangular channel:

$$d_{hG,\Delta} = \frac{4A}{P} = \frac{2bh}{(2s + b)} \quad (18)$$

where A (m²) is cross-sectional area, and P (m) is wetted perimeter of gas or vapor flow channel. Namely, rigorously speaking, the so-called wetted perimeter includes all surfaces acted upon by the shear stress^{13,14}, and this, as recognized long ago by Zogg⁷, also occurs at the crossings of gas flow channels oriented in opposite direction to the extent depending on corrugations inclination angle.

One should note that, in deep vacuum applications, the specific liquid load is rather low, and the corresponding value of film thickness is so small that it can be considered negligible. However, in a theoretically founded approach, all relevant parameters need to be included accordingly. Assuming uniform liquid distribution, i.e., constant film thickness, following expression^{4,5} describes hydraulic diameter of a wetted triangular flow channel:

$$d_{hG} = \frac{(bh - 2\delta s)^2}{\left[\left(\frac{bh - 2\delta s}{2h} \right)^2 + \left(\frac{bh - 2\delta s}{b} \right)^2 \right]^{0.5} + \frac{bh - 2\delta s}{2h}} \quad (19)$$

This definition of hydraulic diameter of an irrigated triangular gas flow channel has been adopted and used with confidence from first publication on DM in 1997⁴. Namely, in practically all applications considered, particularly those concerning design point conditions, gas or vapor ascended through an irrigated bed under turbulent flow conditions. Moreover, practical experiences with various noncircular ducts have confirmed that hydraulic diameter formulation approach, as generally adopted in practice ($d_h = 4A/P$), is surprisingly accurate, within ± 15 %, for turbulent flow¹³.

However, this hydraulic diameter approximation is considered by fluid dynamics theoreticians as relatively crude in laminar flow (± 40 %) ¹³. For-

tunately, for a number of noncircular ducts of commercial interest, including an isosceles triangle, laminar friction constants have been derived analytically, and these ensure best achievable accuracy.

Gas-liquid friction factor

In original DM, only the turbulent flow friction factor was considered^{4,5}. Presently, extended version also includes laminar flow region friction, and overall gas-liquid friction factor is expressed as geometric mean of individual, laminar and turbulent flow friction factors:

$$\xi_{GL} = \sqrt{\xi_{GL,l}^2 + \xi_{GL,t}^2} \quad (20)$$

with

$$\xi_{GL,t} = \left\{ -2 \log \left[\frac{\left(\frac{\delta}{d_{hG,\Delta}} \right) - \frac{5.02}{Re_{Grv}}}{3.7} \right] \cdot \log \left(\frac{\left(\frac{\delta}{d_{hG,\Delta}} \right) + \frac{14.5}{Re_{Grv}}}{3.7} \right) \right\}^{-2} \quad (21)$$

and

$$\xi_{GL,l} = \frac{52.7}{Re_{Grv}} \quad (22)$$

where $\xi_{GL,t}$ (–) is the turbulent gas or vapor flow friction factor, with the relative roughness represented by the ratio of film thickness, δ (m), and the hydraulic diameter of closed triangular gas flow channel, $d_{hG,\Delta}$ (m), and $\xi_{GL,l}$ (–) is the laminar gas flow friction factor. The given laminar friction constant value of 52.7 is an average value covering the range of interest, expressed in terms of apex (fold) angle, ranging from 53.0 at low end (75°) to 52.3 at high end (95°), as taken from a table covering whole apex angle range (0 to 180°)¹³.

Both turbulent and laminar friction factors are expressed as a function of Reynolds number based on relative gas velocity:

$$Re_{Grv} = \frac{(u_{Ge} + u_{Le}) \rho_G d_{hG,\Delta}}{\mu_G} \quad (23)$$

where u_{Ge} (m s⁻¹) and u_{Le} (m s⁻¹) are the effective velocities of the gas and liquid, as defined by Eqs. (9) and (10), respectively.

Gas-gas friction factor

Experiments carried out with air-water and under total reflux with first generation of corrugated sheet structured packings, have indicated that the gas-gas interaction related pressure drop is so

strongly affected by corrugation inclination angle that effects of gas and liquid loads can be neglected. Therefore, in DM, a simple empirical correlation was adopted⁴.

$$\xi_{GG} = 0.722(\cos\alpha)^{3.14} \quad (24)$$

It is based on experiments carried at that time with imperforated Montz B1 type packings with corrugation inclination angles of 45° and 60°, and reflects observed difference in pressure drop that over the whole range of operating conditions was approximately factor 3¹². Note that, in the case of imperforated corrugated sheets, there is no possibility for ascending gas than to follow the V-shaped channels, while in case of perforated packings with common 45°, the gas can ascend under an effective angle larger than 45°, to the extent depending on the form and void fraction of perforations.

Gas flow-direction change losses

Gas flow ascending through a dry or irrigated bed experiences pressure losses due to flow direction change that occurs at transitions between packing layers (bulk), as well as additional pressure loss due to change in flow direction for all channels ending at column walls. Relative magnitude of bulk and wall zone contributions depends on column diameter, packing element height, and corrugation inclination angle. A detailed elaboration on this component of pressure drop can be found in a paper addressing experimental characterization and modelling of column diameter effect¹⁵.

The characteristic pressure loss coefficient is defined as:

$$\zeta_{DC} = \frac{h_{pb}}{h_{pe}} (\xi_{bulk} + \psi \xi_{wall}) \quad (25)$$

where h_{pb} (m) is packed bed height, h_{pe} (m) is packing element or layer height, while ξ_{bulk} (–) and ξ_{wall} (–) represent pressure loss due to direction change related losses at transition between packing elements (bulk of the packing), and in the wall zone, respectively. The fraction of gas flow channels ending at the column walls, ψ (–), depends on the packing element height, corrugation inclination angle, and the column diameter, d_c (m):

$$\psi = \frac{2h_{pe}}{\pi d_c^2 \tan\alpha} \left(d_c^2 - \frac{h_{pe}^2}{(\tan\alpha)^2} \right) + \frac{2}{\pi} \arcsin \left(\frac{h_{pe}}{d_c \tan\alpha} \right) \quad (26)$$

According to this analytically derived expression, the fraction of flow channels ending at column walls becomes 1 for a 45° corrugation inclination angle when the internal column diameter is equal to packing element height, which is approximately 0.2

m for corrugated sheet metal structured packings manufactured in Europe. In case of the same packing but a steeper corrugation inclination angle, i.e., 60° with respect to horizontal, the wall zone is narrower, i.e., the fraction of flow channels ending at column walls becomes 1 at a column diameter of 0.15 m. These values set the lower limit of the validity of Eq. (26) with respect to column diameter.

For bulk flow, the dominating effect is due to angle of change in flow direction at the transition between packing elements or layers,

$$\xi_{bulk} = 1.76(\cos\alpha_{DC})^{1.63} \quad (27)$$

The characteristic angle for the bulk flow is the flow direction-change angle, which, in case of advanced packings with a bend on the ends of corrugations, may be taken as arithmetic mean of corrugation inclination angle and the vertical:

$$\alpha_{DC} = \left(\frac{\alpha + 90^\circ}{2} \right) \quad (28)$$

For the wall zone, the characteristic flow direction-change angle is simply the corrugation inclination angle, α (°). In the wall zone, where wall wipers facilitate buildup of liquid, the pressure drop is also affected by the specific liquid load, u_{LS} (m s⁻¹), as well as the gas velocity and the flow channel hydraulic diameter, the latter two contained in the Reynolds number based on effective gas velocity, Re_{Ge} (–):

$$\xi_{wall} = \frac{4092u_{LS}^{0.31} + 4715(\cos\alpha)^{0.445}}{Re_{Ge}} + 34.19u_{LS}^{0.44}(\cos\alpha)^{0.779} \quad (29)$$

Contribution of wall zone expression depends on the fraction of flow channels ending at column walls, and this, according to Eq. (26), tends to decrease with increasing column diameter.

With this, all working expressions of the DM have been reviewed and explained in detail where needed. The specific pressure drop, i.e., the pressure drop per unit bed height, can simply be obtained by dividing the value estimated by Eq. (4) or Eq. (8) by the bed height:

$$\left(\frac{\Delta p}{\Delta z} \right) = \left(\frac{\Delta p}{h_{pb}} \right) \quad (30)$$

Division by 100 delivers estimated pressure drop in mbar m⁻¹, which is a more convenient unit.

Since experimental data for deep vacuum applications (vapor densities below 0.05 kg m⁻³) are

not available in public domain, the extended DM will be validated using SULCOL predictions as a reference.

DM validation

To demonstrate reliability and predictive accuracy of extended DM, using SULCOL predictions for given Mellapak and BX packings as reference, the nominal specific geometric areas of these packings have been used to determine characteristic dimensions of corrugation base length, corrugation side length, and corrugation height, assuming that the apex or fold angle for Mellapak packings is 90°, while that for BXPlus is 79°. The characteristic numbers are given for generic counterparts of these packings denoted M250.45, MP250.45, M250.60, and BXP in Table 2. Note that actual dimensions of Mellapaks and BXPlus may differ from given numbers, but not significantly. Although different to a lesser extent, packing element heights are taken uniform, as well as porosity for Mellapaks, and the numbers concerning BXPlus also do not differ significantly from the actual ones. Note that all these parameters are required, i.e., taken explicitly into account in DM.

To avoid misunderstandings, the SULCOL predictions are related to Mellapak 250.Y, Mellapak-Plus 252.Y, Mellapak 250.X, and BXPlus as contained in SULCOL database, while DM predictions are related to generic counterparts of these packings denoted in what follows as M250.45, MP250.45, M250.60, and BXP.

Before making any comparisons, it should be noted that validity of drag coefficients and SULCOL pressure drop model predictions is generally set to column diameters from 1 m onward. Spiegel and Duss¹⁰ mention that, in SULCOL, the column diameter effect is accounted for by a correction. Be-

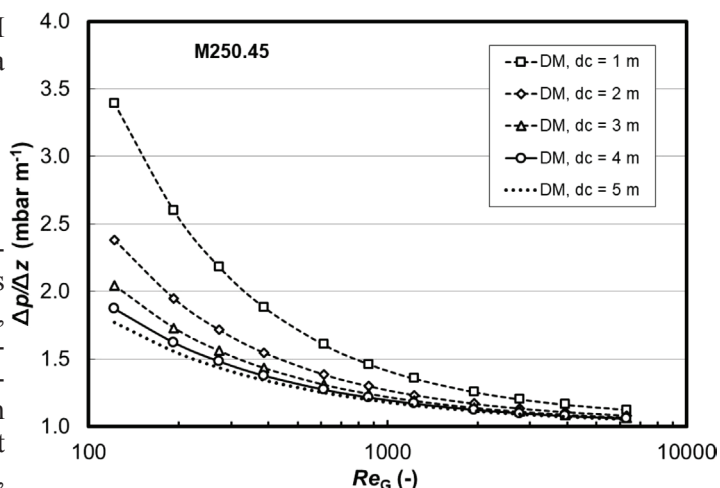


Fig. 5 – Effect of column diameter on specific pressure drop of original DM for most conventional type and size of corrugated sheet structured packing, over the whole range of Reynolds numbers for the hypothetical operating conditions base case

ing proprietary, this information, however, is not readily available to public domain.

DM accounts for diameter effect by the complex empirical expression, i.e., Eq. (25), including Eqs. (26), (27), and (29), developed and validated using experimental pressure drop data obtained with air/water at ambient conditions using columns with internal diameters from 0.2 m to 1.4 m, indicating that observed column diameter effect is evident and needs to be accounted for properly in columns with diameters below 1 m¹⁵. However, when applied to the hypothetical case reflecting deep vacuum operation conditions considered in present work, DM exhibited some peculiar behavior indicating a much stronger column diameter effect than anticipated within the range of low Reynolds numbers ($Re_G < 1000$). This is illustrated, using M250.45 as an example of most conventional structured packing geometry, in a graph shown in Fig. 5 for original model (no laminar friction included). Indeed, as shown in Fig. 5, the effect is rather strong within laminar flow region, and with increasing Re number tends to diminish and fades away at a diameter of 4 m. For this reason, i.e., to have the same basis for comparison with SULCOL results, DM verification calculations have been performed for a column with a diameter of 4 m.

Such a strong column diameter effect within laminar region, which, as shown later, is further enlarged by inclusion of laminar friction expression, could be considered as a kind of anomalous behavior, due to the reasons mentioned previously, i.e., an excessive gas or vapor velocity, which exceeds largely those encountered at same gas or vapor densities in deep vacuum applications. As mentioned previously, industrial columns in such applications operate at F-factors that are factor four lower than

Table 2 – Geometric features of structured packings considered in this study

Geometry	Packing type			
	M250.45	M250.60	MP250.45	BXP
b (m)	0.0226	0.0226	0.0226	0.0103
h (m)	0.0113	0.0113	0.0113	0.0062
s (m)	0.0160	0.0160	0.0160	0.0080
a_p (m ² m ⁻³)	250	250	250	500
ε (m)	0.98	0.98	0.98	0.94
α (°)	45	60	45	60
h_{pe} (m)	0.2	0.2	0.2	0.16
β (°)	90	90	90	79

that employed in present hypothetical base case. The “wrongdoer” in this case of particular hypothetical operating conditions is the empirical expression on the left hand side of Eq. 29, including rather small values of Reynolds number in the denominator ($Re_G < 100$) that delivers unrealistically high values of the correction factor for the wall zone effect, ζ_{wall} (-). Namely, in database used to validate original DM, there were experimental data for air/water and some well-established organic test mixtures available that cover common applications of structured packings where turbulent vapor flow conditions prevail. In all these applications, gas or vapor Reynolds numbers were above 1000, and the extent of increase in pressure drop with decreasing column diameter was experimentally validated¹⁵. An evaluation of most recent experimental evidence, considered further in this paper, has confirmed that observed strongly exaggerated diameter effect is an artefact of the hypothetical base case, i.e., of no practical relevance.

To understand properly the extent of change introduced into DM by incorporating a theoretically founded expression for laminar friction, i.e., Eq. 22, Fig. 6 shows comparison of total and individual pressure loss coefficients for original (DM-old) and extended (DM-new) Delft model. Note that, in the case of original model, the contribution of gas-liquid friction (“GL”) at lowest Reynolds numbers is lower than that of gas-gas interaction or friction (“GG”) and flow direction change (“DC”). While under laminar flow conditions, gas-gas friction plays a significant role⁷, there is no form drag, and consequently the direction change losses do not exist as such, but flow direction change under laminar flow conditions, as mentioned previously, induces some other minor losses.

However, with a constant gas-gas friction coefficient and an appropriate trend in curves representing direction change and gas-liquid friction losses, the total (“TOT”) pressure loss coefficient exhibits expected trend capturing properly laminar and turbulent flow region related behavior. Namely, the trend is similar to that of the SULCOL pressure-drop model drag coefficient, represented by a curve shown as dashed line in Fig. 6. However, the increase in characteristic values is pronouncedly steeper within laminar region than is the case with the curve obtained by original Delft model (DM-old).

The insufficiency of original DM in this respect is mended by including the laminar friction into the model. The triangles connected by solid line show the trend and absolute value of gas-liquid friction coefficient, which start to diverge from original curve at Reynolds number value of 1000, and exhibit much steeper increase than the original one

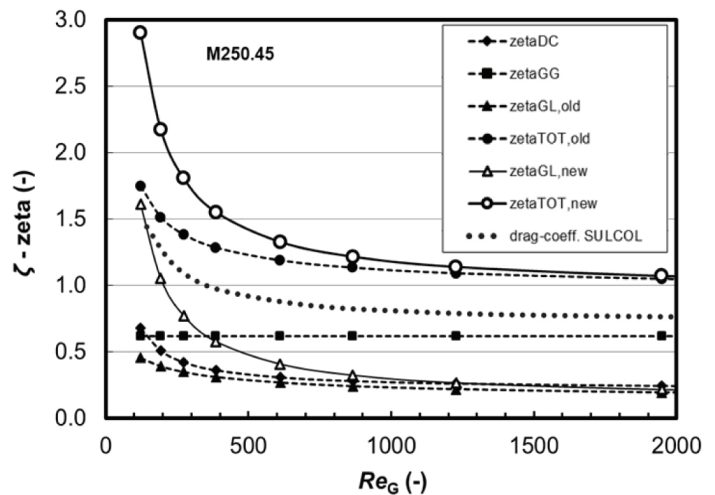


Fig. 6 – Individual and overall pressure loss coefficients for original (symbols with dashed lines) and extended DM (symbols with solid lines), and the corresponding drag coefficient curve of SULCOL (dotted line) for hypothetical base case and M250.45 packing

with decreasing Reynolds number. With this, the laminar friction becomes dominating source of pressure loss within laminar flow region, and this is reflected also in the curve representing total pressure loss coefficient. Differences in characteristic values indicate the extent of expected increase in predicted pressure drop within laminar flow region, which is largest at lowest Reynolds number value (70 %) and tends to decrease steadily, becoming negligible within transition region, and diminishing fully upon entering the turbulent region.

Regarding the fact that the trend of the new line is the same as that of drag coefficient line of SULCOL, we may consider extended DM as properly validated qualitatively. This was the case with all other packings considered, and, as shown in Fig. 7, the predicted pressure drop curves exhibit same trend as those estimated using SULCOL (see Fig. 2). Note that pressure drop is shown as a function of gas or vapor Reynolds number, which differs depending on the type and size of the packing, i.e., hydraulic diameter of gas flow channel. In the case of DM, the characteristic Reynolds numbers are equal for M250.Y and MP252.Y, somewhat lower for M250.X due to a reduced effective gas velocity, and lowest for BXPlus, because of a factor 2 lower value of hydraulic diameter. In the case of SULCOL, the corresponding Reynolds numbers are somewhat larger, due to larger hydraulic diameters employed. They are equal for M250.Y, M250.X, and M252.Y, because hydraulic diameters are equal and superficial velocity is used in definition of characteristic Reynolds number. Due to the differences in the values of hydraulic diameter, there is a certain shift in characteristic Reynolds number

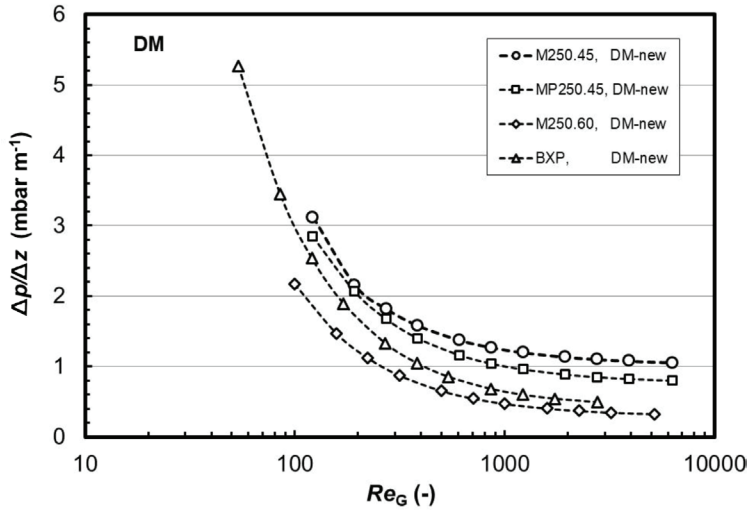


Fig. 7 – Specific pressure drop as estimated by extended DM (DM-new) for four structured packings considered in present study in conjunction with given hypothetical base case

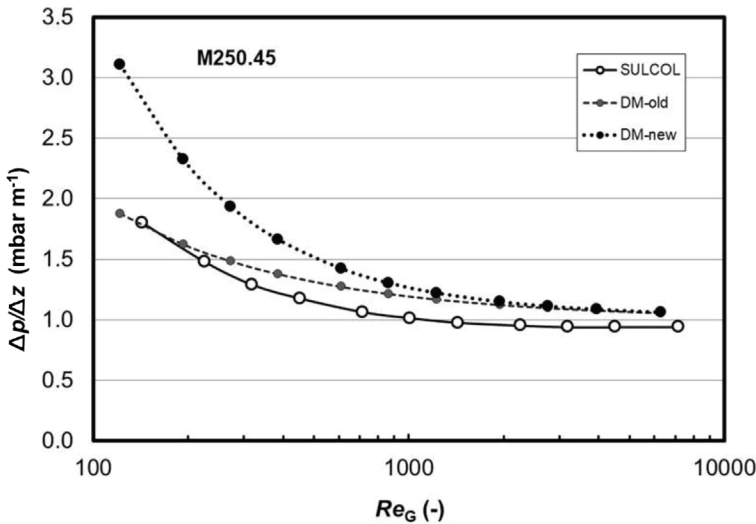


Fig. 8 – Specific pressure drop as estimated by original (DM-old) and extended DM (DM-new) for conventional corrugated sheet structured packing (M250.45) in conjunction with given hypothetical base case, compared with SULCOL estimates for Mellapak 250.Y

points in all graphs comparing predictions of DM with SULCOL results.

Indeed, qualitatively, the predictions of extended DM agree perfectly with SULCOL; however, quantitatively, there are some pronounced discrepancies. If we consider the spread of four curves, the width of the band within turbulent flow region, reflecting the corrugation inclination angle effect, is considerably larger according to DM than SULCOL. This, as well as other quantitative aspects of extended DM (DM-new) using SULCOL results for Mellapak 250.Y, Mellapak 250.X, MellapakPlus 252.Y, and BXPlus as reference, are discussed in detail in following section.

Results and discussion

Hypothetical base case results

Fig. 8 compares predictions of original (DM-old) and extended (DM-new) Delft model with SULCOL curve for Mellapak 250.Y (M250.Y). In this, as well as in other graphs, the original and extended DM curves overlap within turbulent region, and divergence starts roughly at a Reynolds number of 2000, and increases steadily with decreasing Reynolds number. At lowest Reynolds number, the original DM matches perfectly with SULCOL, and extended DM overpredicts SULCOL by nearly 70 %. With increasing Reynolds number, the DM curves exhibit a strong converging trend, overlap upon entering turbulent region, and tend to come closer to that of SULCOL. At highest Reynolds number, the predictions of DM are some 12 % higher than SULCOL values.

MellapakPlus 252.Y (MP250.45) has the same specific geometric area and corrugation inclination angle as Mellapak 250.Y (M250.Y), and its characteristic feature is a short bend at lower and upper end of corrugations. Fig. 2 indicates that, according to SULCOL, the reduction of pressure drop with respect to conventional counterpart ranges from 7 % in laminar- to 19 % in turbulent region, making proper distinction with respect to magnitude of flow regime-related gas-flow direction change contribution.

Comparison of SULCOL curve with those predicted using original and extended DM is shown in Fig. 9. It is amazing to see that the original DM (DM-old) matches nearly perfectly with SULCOL. Extended DM (DM-new) generates much higher pressure drop within laminar region, and at lowest Reynolds number the deviation with respect to SULCOL and DM-old is approximately 75 %, which, however, diminishes fast with increasing Reynolds number, and fades away fully upon reaching turbulent flow region. However, one should mention here that, in addition to proper flow-direction change angle, in the present case, the contribution of gas-gas friction has also been reduced by 20 %. Dotted line represents pressure drop values obtained in case of extended DM without this correction, indicating that, without the gas-gas friction reduction, the pressure drop would be significantly higher, and the discrepancy within laminar (~5 %) and turbulent (~15 %) regions would be somewhat higher. Similar to SULCOL, for this packing, extended DM predicts a smaller pressure drop difference within laminar flow region (9 %) that grows up to 30 % in turbulent region, compared to conventional M250.Y packing. The latter is for largest part due to reduction in pressure drop imposed by a 20 % reduction in contribution of gas-gas interaction.

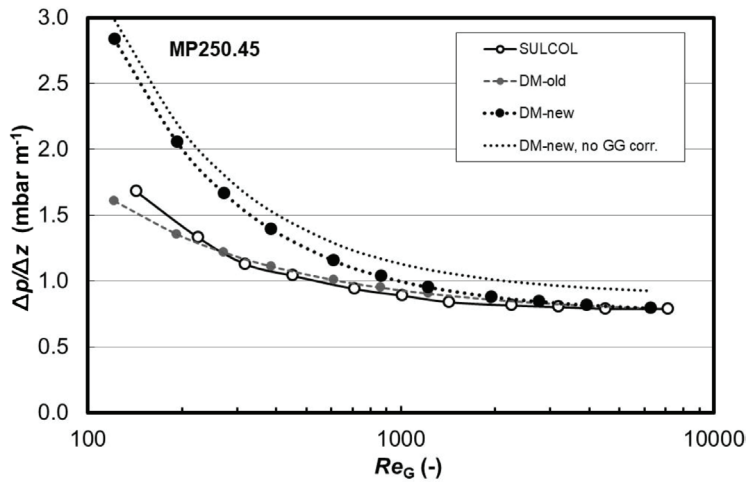


Fig. 9 – Specific pressure drop as estimated by original (DM-old) and extended DM (DM-new) for advanced corrugated sheet structured packing (MP250.45) in conjunction with given hypothetical base case, compared with SULCOL estimates for MellapakPlus 252.Y

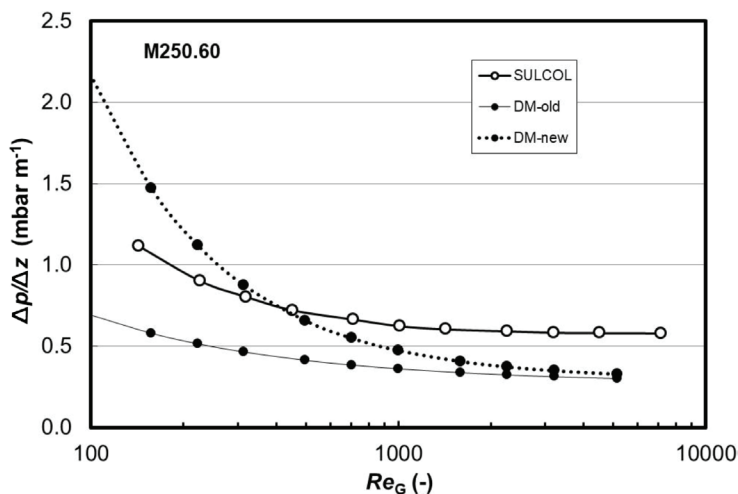


Fig. 10 – Specific pressure drop as estimated by original (DM-old) and extended DM (DM-new) for conventional structured packing with a steep corrugation inclination angle (M250.60) in conjunction with given hypothetical base case, compared with SULCOL estimates for Mellapak 250.X

Now, the question is whether such a simple intervention (multiplying Eq. 20 by an appropriate factor) is justified in this case. The reply is yes, because the smooth bend at lower end of corrugations eliminates the first two to three crossings of neighboring flow channels, and these are in case of conventional 45° packings responsible for most intensive interaction of crossing gas flow streams. In that case, the neighboring flow channels are oriented perpendicular to each other, and at the plane where two gas flows come into contact with each other under the same angle, they exhibit a strong shear stress on each other. This affects both flows and by superimposing motion perpendicular to axial flow direction, both flows start to transform from axial

into a swirling motion. Therefore, at each next crossing plane, the impact angle decreases as well as the amount of shear stress, so that the amount of shear stress and related pressure drop tend to decrease progressively from a maximum at the bottom to a minimum at the top of a flow channel.

In other words, by a delayed start of gas-gas interaction in a packing with smooth bends, total contribution of this pressure loss component reduces to a certain extent. In the present, 45° (worst) case, this has been taken to be 20 %, but this is an arbitrary choice, and someone may consider another percentage more appropriate or better fitting own situation. Such a correction may appear unnecessary in the case of packings with specific geometric areas of $500 \text{ m}^2 \text{ m}^{-3}$ or more, because of much larger channel length to hydraulic diameter ratio than in the case of common size packings. In any case, 60° packings with smooth bends on both, like BXPlus, or only lower end of corrugations, like Montz A3-500M, will not be affected significantly in this respect. Therefore, in the case of BXP packing, the GG interaction reduction correction was not utilized.

As illustrated in Fig. 10, in the case of the common size packing with a much steeper corrugation inclination angle (M250.60), the original DM approaches closely SULCOL values within laminar region. Here, the overprediction at lowest Reynolds number of extended DM is even larger, but it reduces strongly and in transient region the two methods overlap. However, within turbulent region, the underprediction tends to increase, reaching some 70 % on high end of Reynolds numbers.

Indeed, as demonstrated in Fig. 10, SULCOL and DM differ strongly with respect to the effect of corrugation or gas flow channel inclination angle. As mentioned previously, the 45° and 60° values differ in the case of SULCOL by a factor 1.62 over the whole range of Reynolds numbers, including both laminar and turbulent flow regions. This, as mentioned previously, is questionable, because within turbulent region, the form drag, particularly that due to sudden direction change at each transition between packing layers, generates a substantial amount of pressure drop in addition to frictional one. This physically more sound picture is reflected by predictions of DM, and in given case, the difference in pressure drop between packings with corrugation inclination angles of 45° and 60° is lower in laminar region (factor 1.45) than within turbulent region (up to factor 3.5). The latter was based on air/water experiments and cyclohexane/n-heptane total reflux experiments carried out with imperforated Montz B1-250 and B1-250.60 packings^{5,12}. Experiments utilizing perforated packings have indicated a less pronounced corrugation inclination

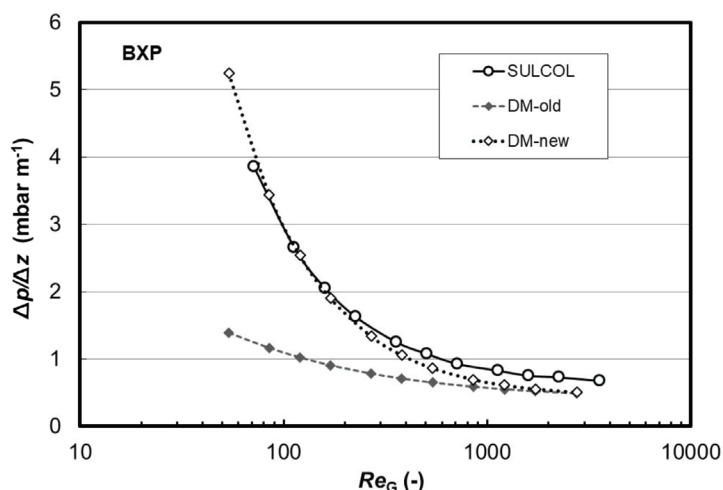


Fig. 11 – Specific pressure drop as estimated by original (DM-old) and extended DM (DM-new) for advanced wire gauze corrugated sheet structured packing (BXP) in conjunction with given hypothetical base case, compared with SULCOL estimates for BXPPlus

angle effect (up to factor 2.5). This reduction was attributed to the fact that in the case of perforated packings with common 45° , the gas can partly use the perforations and ascend under an effective angle larger than 45° , while in the case of imperforated packings, ascending gas or vapor is forced to flow strictly along the V-shaped flow channel.

While the extent of pressure drop overprediction in the case of conventional perforated corrugated sheet structured packings with corrugation inclination angle of 45° (M250.Y) can be considered comfortable (it is on safe side and the amount is within common safety margins), the demonstrated underprediction in the case of 60° packing (M250.X) is too strong to be considered acceptable. This is a point of concern, but in the present case, the observed discrepancy is with respect to values estimated by SULCOL, which suggests that the corrugation inclination angle effect is half of that which has been established in aforementioned experiments with imperforated and perforated Montz packings.

Interestingly, in the case of another 60° packing considered in present study, i.e., BXP (see Fig. 11), the underprediction of DM is much less pronounced, up to 33 % at largest Reynolds number. The overprediction on lowest Reynolds number is around 35 % and diminishes strongly, and within laminar and transient range the curves nearly overlap, indicating a very good agreement between extended DM and SULCOL for this type of structured packing. Note that in this case, the original DM was insufficient, and by incorporating the laminar friction term, the pressure drop estimates have been brought to the level attainable by SULCOL.

For practitioners, it may appear worrying that at lowest Reynolds number considered here, the ex-

tended DM exceeds SULCOL and generates a pressure drop well above 3 mbar m^{-1} for BXP packing. However, as mentioned previously, this is an anomaly of no practical consequence, related to the choice of fixed value of F-factor ($F_G = 2 \text{ Pa}^{0.5}$) for this hypothetical operating conditions base case. To keep pressure drop within tolerable limits, the diameters of industrial columns for deep vacuum applications are chosen to be large enough to reduce superficial gas or vapor velocity accordingly. Such columns usually operate at F-factors of around $0.5 \text{ Pa}^{0.5}$. Owing to their favorable wetting characteristics at lowest specific liquid loads that facilitate achieving highest separation efficiency at lowest pressure drop, conventional as well as advanced forms of wire gauze corrugated sheet structured packings are a natural candidate for deep vacuum distillation. This has been proven in numerous industrial applications. What is still missing, to enable proper validation of theoretically founded predictive models for these purposes, is availability of adequate experimental evidence in public domain.

Large-scale total reflux tests data

Unfortunately, there is no experimental evidence available in public domain on performance of structured packings in deep vacuum applications where laminar flow prevails, such as, steam stripping of edible oils. Nevertheless, there is some scarce experimental evidence available in open literature that could be revealing in this respect to a limited extent. Namely, lowest vapor loads employed in total reflux distillation tests, carried out at Bayer TS with Montz A3-500 and A3-500M wire gauze corrugated sheet structured packings¹⁶, provide experimental evidence on performance of conventional and advanced geometries under same operating conditions, including a few points where, according to characteristic Reynolds number, the ascending vapor flow ought to be laminar. These data were used to validate original Delft Model, and, most interestingly, shed some light on the effect of smooth bend in the bottom of corrugations on pressure drop within laminar and turbulent flow regions.

Fig. 12 shows preloading region pressure drop as a function of vapor load, as determined for A3-500M, an advanced wire gauze packing with a long smooth bend in bottom part of corrugations (a Montz equivalent of Sulzer BXPlus), and its conventional counterpart A3-500 in total reflux distillation experiments carried out at BTS using a column with internal diameter of 0.59 m and chlorobenzene-ethylbenzene as test system at 0.1 bar¹⁶. Within the laminar region ($Re_{Gs} < 400$, i.e. $F_{Gs} < 0.75 \text{ Pa}^{0.5}$), the pressure drop curves overlap, and in transient region, a divergent trend sets up that tends to

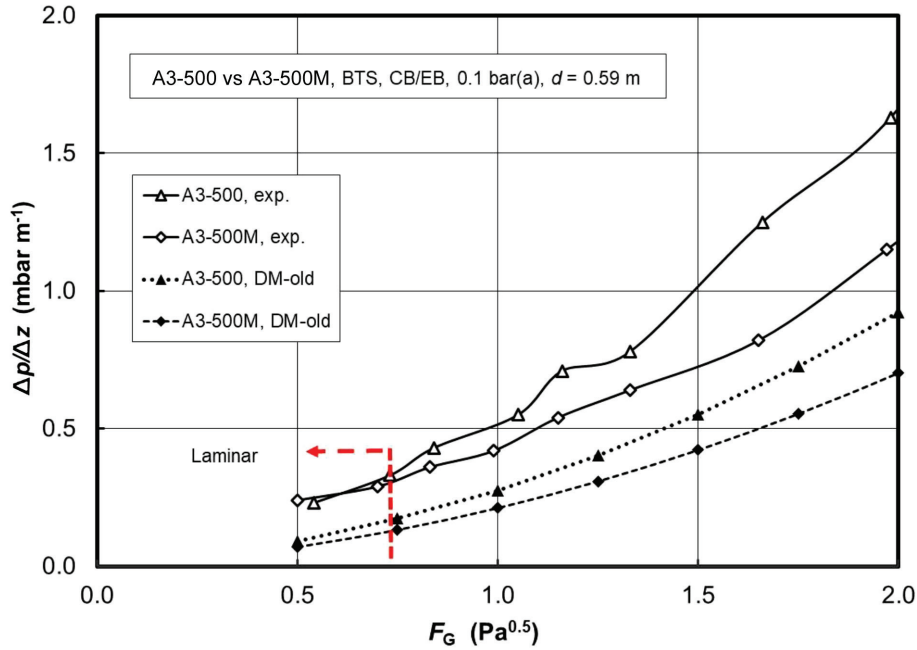


Fig. 12 – Effect of a bend in bottom part of corrugations on the pressure drop of a well-established wire gauze corrugated sheet structured packing, as measured in total reflux tests carried out at Bayer Technology Services, using chlorobenzene/ethylbenzene system at 0.1 bar¹⁶. Dotted and dashed lines are predictions by original DM, and laminar flow should prevail at F -factors below $0.75 \text{ Pa}^{0.5}$.

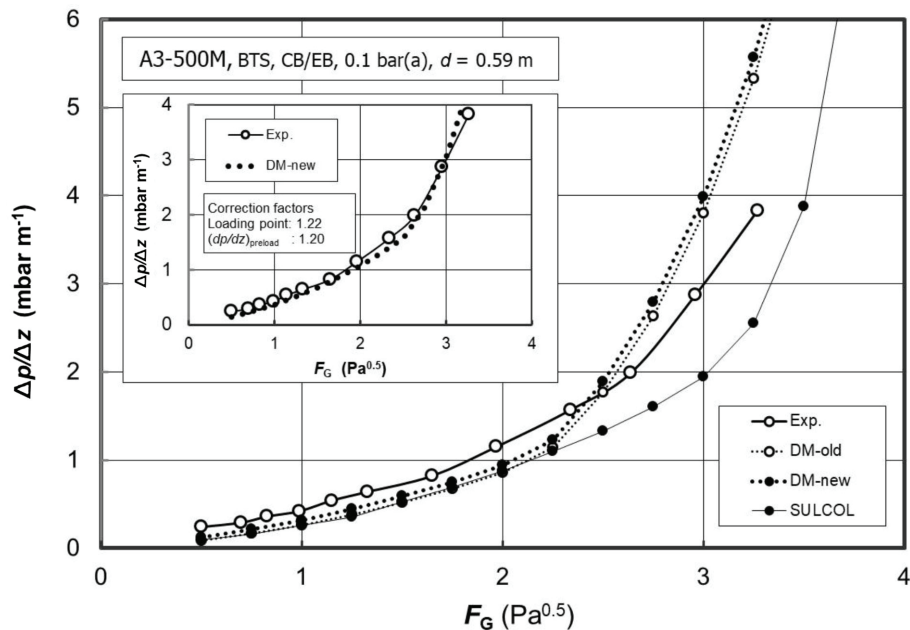


Fig. 13 – Comparison of the specific pressure drop as estimated by original (DM-old) and extended DM (DM-new) for advanced wire gauze corrugated sheet structured packing A3-500M compared with experimental data (BTS, 0.1 bar). SULCOL estimates are related to BXPlus. Inset graph demonstrates that pressure drop predicted by extended DM utilizing two correction factors, which reflect the extent of deviation in this case, perfectly matches with experiment.

grow further within turbulent flow region, with conventional packing pressure drop on higher side. This indicates that advanced geometry with a smooth bend on bottom end of corrugations is not effective within laminar region where only friction-

al pressure drop counts, while within the turbulent region, it minimizes the flow-direction-change related form drag, and reduces the overall pressure drop to a greater extent compared to that of the conventional counterpart. Regarding the fact that in this

case the corrugation inclination angle is rather steep (60°), the extent of reduction in pressure drop as observed with A3-500M within turbulent region is quite impressive. However, a part of it can be attributed to somewhat lower specific geometric area ($478 \text{ m}^2 \text{ m}^{-3}$) compared to that of A3-500 ($490 \text{ m}^2 \text{ m}^{-3}$)¹⁶.

It is interesting to mention here that, in these low specific liquid load cases, no visible capacity gain was observed; however, if one takes a fixed pressure drop as design criterion, then a column of the same diameter, equipped with A3-500M, can be operated at 10 % higher vapor throughput.

As illustrated in Fig. 12, original DM reproduces very closely the observed trends, but predicted pressure drop values within preloading region are on the low side, practically speaking, too optimistic.

In Fig. 13, predictions of original (DM-old) and extended DM (DM-new) for A3-500M, and those obtained by SULCOL for BXPlus, are compared with experimental pressure drop curve for A3-500M. This graph is of particular importance, because it demonstrates that incorporation of laminar friction enhances predicted pressure drop at lowest Reynolds numbers significantly with respect to that obtained using original model (dotted lines). However, the predicted values are still well below experimental ones, obtained using a test column with an internal diameter of 0.59 m. This indicates that a very strong column diameter effect exhibited in the hypothetical case (see Fig. 5) within laminar region appears to be unrealistic, i.e., of no consequence for performance of DM in common applications.

Interestingly, the curve obtained using original DM, which follows the trend of the measured curve, overlaps within preloading region with that predicted by SULCOL for BXPlus packing. This is not a coincidence, as shown later, and may be considered as quite convincing proof that incorporation of laminar friction has resulted in a physically sound amount of pressure drop enhancement within laminar flow region, leading to improvement in overall pressure drop estimation performance of DM within preloading region.

Unfortunately, comparison of predicted and experimental pressure drop curves shown in Fig. 13, indicates a worrying degree of underprediction of loading point. Therefore, the pressure drop enhancement expression in DM (Eq. 5) accounting for observed, much steeper increase in pressure drop with increasing vapor load within loading region, is activated at a too low vapor load, which leads to a strong overprediction of pressure drop within loading region. To indicate the extent of enhancement in pressure drop with increasing vapor load within loading region, the preloading curve for original

DM extends into loading region. This curve follows that of SULCOL valid for BXPlus until the point of departure in pressure drop according to SULCOL, which is more realistic than that predicted by DM.

Most importantly, the trends in predicted pressure drop by original and extended DM for both preloading and loading regions are correct, and with a properly predicted loading point, the deviation in predicted pressure drop within loading region would be similar to that of SULCOL on lower side but within the acceptable limits. As demonstrated in small graph inserted into main graph in Fig. 13, using another single correction factor, for underpredicted pressure drop within preloading region, would ensure a perfect match between predicted and measured pressure drop curves.

Impressions gained from the comparisons shown in Fig. 13, have been strengthened upon validation of extended DM using experimental evidence on A3-500M performance, obtained most recently in Fractionation Research Inc. (FRI) total reflux distillation tests carried out with *p*-xylene/*o*-xylene system at absolute pressures of 0.1 bar and 0.02 bar in a column with internal diameter of 1.22 m¹⁷. As illustrated in Figs. 14 and 15, inclusion of laminar friction term has increased the estimated pressure drop within preloading region significantly with respect to original method; however, the predicted values are still well below the measured ones.

In these cases, a nearly perfect match is obtained between extended DM and SULCOL within preloading region, and, regrettably, DM exhibited an even larger extent of underprediction of loading point compared to that experienced in BTS test. SULCOL provided correct estimates for loading point, and a tendency to approach the measured pressure drop within loading region from lower side. Again, utilizing correct value for loading point, the pressure drop curve predicted by extended DM would be similar to that of SULCOL, and similar to the situation shown in Fig. 13, only one additional correction factor for preloading region pressure drop is required to obtain nearly perfect match over the whole range of vapor loads. This is demonstrated in small graphs inserted in main graphs shown in Figs. 14 and 15, respectively.

The comparison of predicted and measured pressure drops shown in Figs. 13, 14 and 15, indicates that existing empirical correlations are incapable of identifying properly the loading point of structured packings with a smooth bend on lower part of corrugations. Another point of concern is related largely to underprediction of preloading region pressure drop of packings with corrugation inclination angle of 60° . Simple empirical correlation accounting for corrugation inclination angle ef-

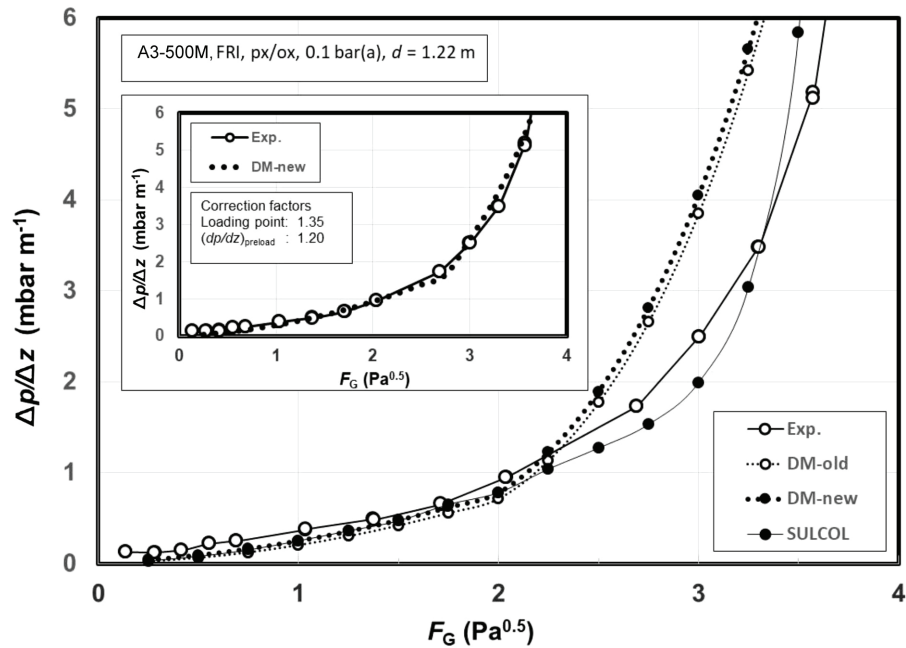


Fig. 14 – Comparison of the specific pressure drop as estimated by original (DM-old) and extended DM (DM-new) for advanced pressure drop as estimated by original (DM-old) and extended DM (DM-new) for advanced wire gauze corrugated sheet structured packing A3-500M compared with experimental data (FRI, 0.1 bar). SULCOL estimates are related to BXPlus. Inserted graph demonstrates that pressure drop predicted by extended DM utilizing two correction factors, which reflect the extent of deviation in this case, perfectly matches with experiment.

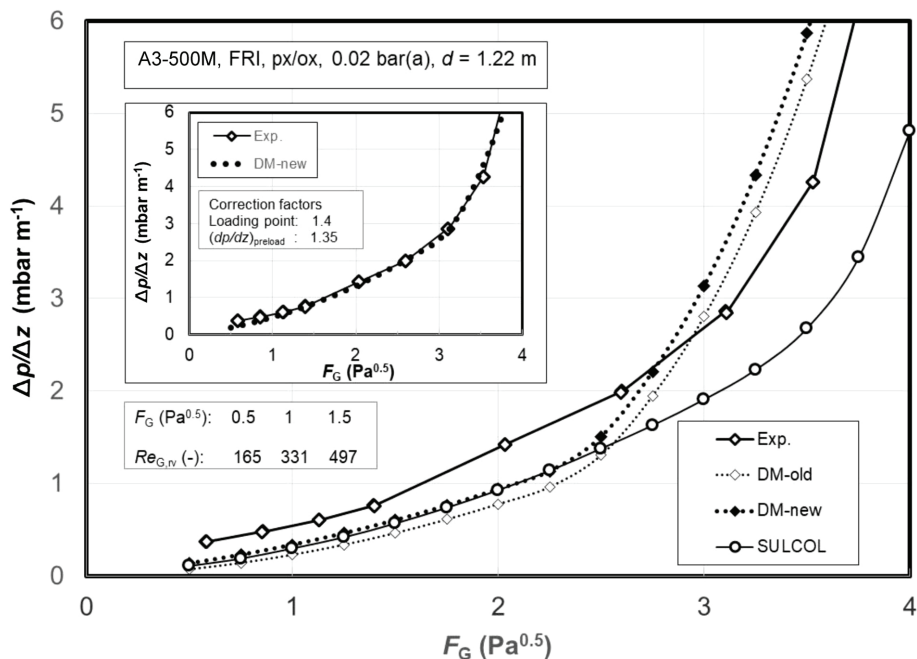


Fig. 15 – Comparison of the specific pressure drop as estimated by original (DM-old) and extended DM (DM-new) for advanced wire gauze corrugated sheet structured packing A3-500M compared with experimental data (FRI, 0.02 bar). SULCOL estimates are related to BXPlus. Inserted graph demonstrates that pressure drop predicted by extended DM utilizing two correction factors, which reflect the extent of deviation in this case, perfectly matches with experiment.

fect on gas-gas interaction at the open interface of crossing gas flow channels appears to be inadequate for packings with steep corrugation inclination angle. A simple check, i.e., reduction of exponent of Eq. 24 by one third, has indicated that, in all cases considered here, the resulting increase in contribution of gas-gas interaction would bring predicted preloading pressure drop at the level of the measured one. However, this is not a solution, because utilizing the same exponent for 45° packings would force gas-gas interaction contribution to rise beyond that considered sound. To arrive at proper solutions in this respect, empirical correlations used in DM for establishing the loading point and the extent of corrugation inclination angle effect need to be thoroughly reevaluated and improved.

Regarding usability, one should mention that corrugation inclination angles of 45° and 60° considered in present study are a manufacturing standard. However, other angles can be considered if there is a need to balance properly the efficiency, pressure drop, and capacity of a packing for a specific application. Corrugation inclination angles as low as 40° have been commercialized, and an intermediate angle found most favorable for structured packings used in air distilling applications¹⁸. In addition, there are corrugated sheet structured packings around utilizing two different angles within the height of a packing layer¹⁹. Note that DM is the only predictive model capable of providing a reliable estimate of pressure drop in such cases, based on form, dimensions, and the inclination angle(s) of gas or vapor flow channel. On higher end, the natural limit is the vertical line, i.e., an angle of 90°, when a corrugated sheet structured packing transforms into a falling film device. DM accounts for this, i.e., the flow direction change and gas-gas interaction contributions drop to zero, and the total pressure drop is equal to frictional pressure drop. Indeed, DM is highly versatile and can easily be adapted or extended to include variations in characteristic geometric features of corrugated sheet structured packings.

Conclusions

Delft model has been extended in a physically sound way to cover the range of lowest vapor and liquid loads, where gas or vapor ascends through an irrigated structured packing bed under laminar flow conditions.

In absence of any experimental data in public domain, a hypothetical base case reflecting closely the deep vacuum distillation conditions, served as basis for validation of extended DM using a well-established empirical pressure drop model available in SULCOL software package as reference.

Four well-known and widely utilized Sulzer corrugated sheet structured packings have been chosen to demonstrate effects of variations in specific geometric area and the corrugation angle, as well as of smooth bends at both ends of corrugations, as encountered in case of high performance versions of conventional corrugated sheet structured packings.

By incorporating a theoretically based formulation of laminar flow friction factor, the predictions of DM approach closely those of SULCOL, both qualitatively and quantitatively in laminar and flow regime transition regions. Trends are also identical within turbulent region; however, discrepancy between two models is more pronounced. DM tends to overpredict the pressure drop in case of 45° packings to an acceptable (safety margin) extent, while the extent of underprediction in case of 60° packings appears to be beyond tolerable limits.

Validation of extended DM using results of large-scale total reflux tests carried out at absolute top pressures of 0.02 and 0.1 bar with Montz A3-500M packing, including few points in laminar flow regime, has indicated a certain extent of underprediction of pressure drop within preloading region, reflecting that observed during hypothetical case evaluations for packings with steep corrugation inclination angle. This confirms the impression that gas-gas interaction related losses in case of 60° packings must be significantly larger than anticipated.

Another point of concern is a pronounced underprediction of loading point for this packing, i.e., wire gauze corrugated sheet structured packings with a smooth bend at the lower end of corrugations, resulting in large overprediction of pressure drop within loading region. With this in mind, the appropriateness of empirical correlations accounting for loading point identification and gas-gas interaction developed in the time before introduction of advanced packings with bends at lower and upper ends of corrugations, will be addressed soon.

Regarding the fact that SULCOL predictions for BXPlus packing match very well with extended DM predictions for A3-500M within preloading region, and reflect both the trend of measured pressure drop within loading region, this evidence confirms reliability of SULCOL as predictive model, and justifies its choice as reference in absence of experimental data in public domain adequate for DM model validation.

ACKNOWLEDGEMENT

Leon Voogd and Hans Poelwijk, now with engineering contractor Fluor for more than 20 years, during their graduation time at TU Delft have performed under supervision of the author, with utmost

care, numerous experiments and finally laid the foundations of pressure drop model, which is well established and generally known in the literature as the Delft Model.

Notation

a_p	– specific geometric area, $\text{m}^2 \text{m}^{-3}$
A	– cross-sectional area, m^2
b	– corrugation base, m
c_f	– drag coefficient, –
d_c	– (dc) column diameter, m
d_{hG}	– hydraulic gas flow channel diameter, m
F_G	– gas (vapor) load factor, $\text{Pa}^{0.5}$
$F_{G,lp}$	– loading point gas load factor, $\text{Pa}^{0.5}$
F_{load}	– loading effect factor, –
g	– gravitational acceleration, m s^{-2}
h	– corrugation height, m
h_L	– liquid holdup, $\text{m}^3 \text{m}^{-3}$
h_{pb}	– height of packed bed, m
h_{pe}	– height of packing element or layer, m
l_G	– length of gas flow path, m
P	– wetted perimeter, m
p	– operating pressure, Pa or bar
Re_{Ge}	– effective gas phase Reynolds number, –
Re_{Grv}	– relative velocity Reynolds number, –
Re_L	– Reynolds number for the liquid, –
s	– corrugation side, m
u_{Ge}	– effective gas velocity, m s^{-1}
u_{Gs}	– superficial gas velocity, m s^{-1}
u_{Le}	– effective liquid velocity, m s^{-1}
u_{Ls}	– superficial liquid velocity, m s^{-1}

Greek letters

α	– corrugation inclination angle, $^\circ$
α_{DC}	– gas flow direction change angle, $^\circ$
α_L	– effective liquid flow angle, $^\circ$
β	– apex or fold angle, $^\circ$
δ	– liquid film thickness, m
δ_m	– sheet thickness, m
Δp	– pressure drop or loss, Pa or mbar
$\Delta p/\Delta z$	– pressure drop per unit bed height, Pa m^{-1} or mbar m^{-1}
ε	– packing porosity, –
φ	– fraction of the triangular flow channel occupied by liquid, –
μ_G	– viscosity of gas, Pa s
μ_L	– viscosity of liquid, Pa s
ρ_G	– density of gas, kg m^{-3}

ρ_L	– density of liquid, kg m^{-3}
σ	– surface tension, N m^{-1}
ζ_{DC}	– overall coefficient for direction change losses, –
ζ_{GG}	– overall coefficient for gas-gas friction losses, –
ζ_{GL}	– overall coefficient for gas-liquid friction losses, –
ζ_{TOT}	– $(\zeta_{GL} + \zeta_{GG} + \zeta_{DC})$ total pressure loss coefficient, –
ζ_{bulk}	– direction change factor for bulk zone, –
ζ_{GG}	– gas-gas friction factor, –
ζ_{GL}	– gas-liquid friction factor, –
ζ_{wall}	– direction change factor for wall zone, –
Ψ	– fraction of gas flow channels ending at column walls, –

Subscripts

G	– gas or vapor
L	– liquid
l	– laminar
rv	– relative velocity
s	– superficial
t	– turbulent
v	– V-shaped flow channel
Δ	– triangular flow channel

References

- Duss, M., Pressure drop prediction at low operating pressure: Is there anything new?, AIChE Spring Meeting, April 2013, San Antonio, Texas, USA, pp. 1–11.
- Faessler, P., Kolmetz, K., Seang, K. W., Lee, S. H., Advanced fractionation technology for the oleochemical industry, A.-PAC J. Chem. Eng. **2** (2007) 315. doi: <https://doi.org/10.1002/apj.025>
- Sulzer Chemtech, Tower Technical Bulletin, Chem. Eng. Progress, August 2013.
- Olujić, Ž., Development of a complete simulation model for predicting hydraulic and separation performance of distillation columns equipped with structured packings, Chem. Biochem. Eng. Q. **11** (1997) 31.
- Fair, J. R., Seibert, A. F., Behrens, M., Saraber, P. P., Olujić, Ž., Structured packing performance: Experimental evaluation of two predictive models, Ind. Eng. Chem. Res. **39** (2000) 1788. doi: <https://doi.org/10.1021/ie990910t>
- Huber, M., Sulzer-Kolonnen für Vakuumrektifikation, Sulzer techn. Rdsch. **49** (1) (1967) 30.
- Zogg, M., Strömungs- und Stoffaustauschuntersuchungen an der Sulzer- Gewebepackung (Thesis, ETH, Zürich), Verlag Hans Stellenberg, Winterthur, 1972.
- Zogg, M., Stoffaustausch in der Sulzer-Gewebepackung, Chemie-Ing.-Techn. **45** (2) (1973) 67.
- Chew Pew Ang, SULCOL™ design program for mass transfer columns, Sulzer Technical Review **100** (3) (2018) 10.

10. *Spiegel, L., Duss, M.*, Structured Packings, Chapter 4 in *Distillation Equipment and Processes* (Editors: A. Gorak and Ž. Olujić), Academic Press/Elsevier, 2014, pp. 145–181.
doi: <https://doi.org/10.1016/B978-0-12-386878-7.00004-8>
11. *Duss, M.*, personal communication, 2014.
12. *Verschoff, H. J., Olujić, Ž., Fair, J. R.*, A general correlation for predicting the loading point of corrugated sheet structured packings, *Ind. Eng. Chem. Res.* **38** (1999) 3866.
doi: <https://doi.org/10.1021/ie990009d>
13. *White, F. M.*, *Fluid Mechanics* (III Edition), McGraw-Hill, 1994.
14. *Truckenbrodt, E.*, *Strömungsmechanik*, Springer Verlag, Berlin, 1968.
15. *Olujić, Ž.*, Effect of column diameter on pressure drop of a corrugated sheet structured packing, *Trans IChemE* **77** Part A (1999) 505.
16. *Olujić, Ž., Rietfort, T., Jansen, H., Zich, E., Frey, G., Ruffert, G., Zielke, T.*, Experimental characterization and modelling of high performance structured packings, *Ind. Eng. Chem. Res.* **51** (2012) 4414.
doi: <https://doi.org/10.1021.ie202585t>
17. *Schulz, R., Rietfort, T., Jansen, H., Olujić, Ž.*, Experimental evidence on performance of an advanced gauze structured packing under deep vacuum distillation conditions, *Chem. Eng. Trans.* **69** (2018) 763.
doi: <https://doi.org/10.3303/CET1869128>
18. US 2013/0233016 A1 (Sep. 12, 2013).
19. *Olujić, Ž., Jödecke, M., Shilkin, A., Schuh, G., Kaibel, B.*, Equipment improvement trends in distillation, *Chem. Eng. Process.* **48** (2009) 1089.
doi: <https://doi.org/10.1016/j.cep.2009.03.004>